

Title: A Low-Cost and Field Portable Electromechanical (E/M) Impedance Analyzer for Active Structural Health Monitoring

Authors: Buli Xu
Victor Giurgiutiu

Paper to be presented at: *5th International Workshop on Structural Health Monitoring, Stanford University, Stanford, CA, September 15-17, 2005*

Report Documentation Page

*Form Approved
OMB No. 0704-0188*

Public reporting burden for the collection of information is estimated to average 1 hour per response, including the time for reviewing instructions, searching existing data sources, gathering and maintaining the data needed, and completing and reviewing the collection of information. Send comments regarding this burden estimate or any other aspect of this collection of information, including suggestions for reducing this burden, to Washington Headquarters Services, Directorate for Information Operations and Reports, 1215 Jefferson Davis Highway, Suite 1204, Arlington VA 22202-4302. Respondents should be aware that notwithstanding any other provision of law, no person shall be subject to a penalty for failing to comply with a collection of information if it does not display a currently valid OMB control number.

1. REPORT DATE 2005	2. REPORT TYPE N/A	3. DATES COVERED -						
4. TITLE AND SUBTITLE A Low-Cost and Field Portable Electromechanical (E/M) Impedance Analyzer for Active Structural Health Monitoring								
5a. CONTRACT NUMBER 								
5b. GRANT NUMBER 								
5c. PROGRAM ELEMENT NUMBER 								
6. AUTHOR(S) 								
5d. PROJECT NUMBER 								
5e. TASK NUMBER 								
5f. WORK UNIT NUMBER 								
7. PERFORMING ORGANIZATION NAME(S) AND ADDRESS(ES) University of South Carolina, Columbia, SC 29208								
8. PERFORMING ORGANIZATION REPORT NUMBER 								
9. SPONSORING/MONITORING AGENCY NAME(S) AND ADDRESS(ES) 								
10. SPONSOR/MONITOR'S ACRONYM(S) 								
11. SPONSOR/MONITOR'S REPORT NUMBER(S) 								
12. DISTRIBUTION/AVAILABILITY STATEMENT Approved for public release, distribution unlimited								
13. SUPPLEMENTARY NOTES The original document contains color images.								
14. ABSTRACT 								
15. SUBJECT TERMS 								
16. SECURITY CLASSIFICATION OF: <table style="width: 100%; border-collapse: collapse;"> <tr> <td style="width: 33%; text-align: center;">a. REPORT unclassified</td> <td style="width: 33%; text-align: center;">b. ABSTRACT unclassified</td> <td style="width: 34%; text-align: center;">c. THIS PAGE unclassified</td> </tr> </table>			a. REPORT unclassified	b. ABSTRACT unclassified	c. THIS PAGE unclassified	17. LIMITATION OF ABSTRACT UU	18. NUMBER OF PAGES 12	19a. NAME OF RESPONSIBLE PERSON
a. REPORT unclassified	b. ABSTRACT unclassified	c. THIS PAGE unclassified						

ABSTRACT¹

This paper presented the implementation of a DAQ card based low-cost impedance analyzer for active structural health monitoring. Two excitation signal sources for efficient and accurate measurement of the E/M impedance are digitally synthesized. The characteristics of these two signal sources for impedance measurement were first compared in simulation and then examined by measuring the impedance spectrum of a free piezoelectric wafer active sensor. Finally, the performance of this novel impedance analyzer was compared to HP4194A impedance analyzer for detecting a disbond on a spacecraft test panel with piezoelectric wafer active sensors.

INTRODUCTION

The electromechanical (E/M) impedance method is a new embedded ultrasonics method that is emerging as an effective and powerful technique for structural health monitoring (SHM)^{[1][2]}. Through PWAS (piezoelectric wafer active sensor) permanently attached to the structure, the E/M impedance method is able to measure directly the high-frequency local impedance spectrum of the structure. Because the high-frequency local impedance spectrum is much more sensitive to incipient damage than the low-frequency global impedance, the E/M impedance method is better suited for applications in SHM than other more conventional methods.

Although PWAS are small, unobtrusive, and inexpensive, the laboratory impedance measurement equipment (e.g., HP4194 impedance analyzer) used in the proof-of-concept demonstration of these technologies is bulky, heavy, and relatively expensive. Several investigators have explored means of reducing the size of the

¹ Graduate Research Assistant, Department of Mechanical Engineering, University of South Carolina, Columbia, SC 29208, xub@engr.sc.edu; 803-777-1535.

² Professor, Department of Mechanical Engineering, University of South Carolina, Columbia, SC 29208, giurgiut@engr.sc.edu; 803-777-8018.

impedance analyzer, to make it more compact, even field-portable^{[3]-[7]}. HP4194A impedance analyzer measures DUT impedance spectrum by exciting step by step pure tones of sinewaves of increasing frequency. The DUT's excitation signal and response signal will then be separated into in-phase part and quadrature part respectively by using sine correlation algorithm implemented in analog circuit, for later complex impedance calculation^[8]. This method requires complicated hardware and needs to record exact integer numbers cycle of sinewaves at each frequency step and is time consuming. This paper discussed the implementation of a low-cost impedance analyzer for active structural health monitoring using two synthesized signal sources for accurate and efficient E/M impedance measurement.

CONCEPT

For a linear system, by transforming the time domain excitation signal (voltage $[v(t)]$) and response signal (current $[i(t)]$) of the DUT to yield the frequency domain quantities $[V(j\omega)]$ and $[I(j\omega)]$, the admittance of DUT may be calculated as the transfer function of DUT^{[9]-[11]} (Figure 1).

$$Y(j\omega) = \frac{I(j\omega)}{V(j\omega)} \quad (1)$$

Hence, the impedance of DUT is

$$Z(j\omega) = \frac{FFT\{v(t)\}}{FFT\{i(t)\}} \quad (2)$$

where, $FFT\{\}$ designates fast Fourier transform. With this concept, the impedance spectrum of a DUT can be acquired even within one wideband excitation signal sweeping.

SINGAL SOURCES FOR E/M IMEPDANCE MEASUREMENT

Linear Chirp Signal

Linear chirp can be synthesized easily in time domain^{[12][13]} (Figure 2a). Consider a general signal $x(t) = \text{Re}\{Ae^{j\phi(t)}\}$, a linear chirp signal is produced when

$$\phi(t) = \pi\beta t^2 + 2\pi f_0 t + \phi_0 \quad (3)$$

Computing the instantaneous frequency, f_i , of the chirp, we have $f_i(t) = \beta t + f_0$. The parameter $\beta = (f_1 - f_0)/t_1$ is the rate of frequency change, which is used to ensure the desired frequency breakpoint f_1 at time t_1 is maintained.

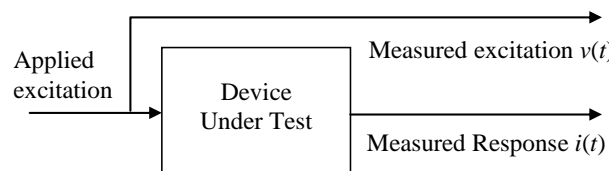


Figure 1 Configuration for impedance measurement using transfer function of DUT¹⁰

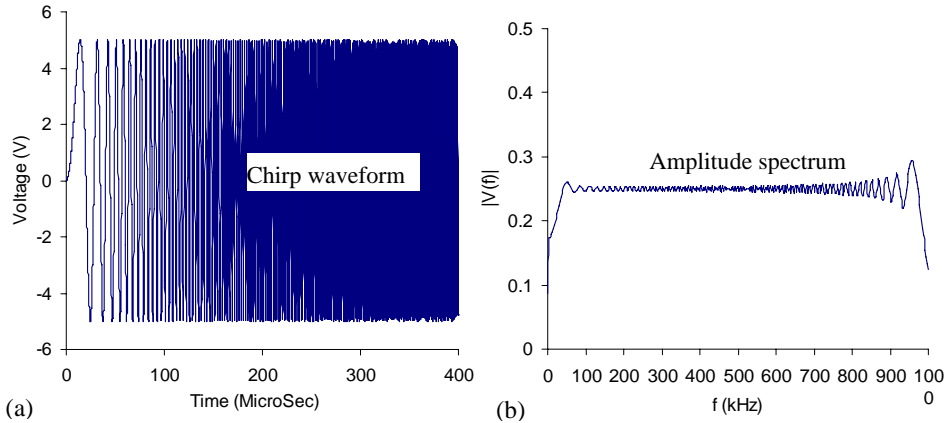


Figure 2 Linear chirp signal (sweep from DC to 1MHz): (a) waveform; (b) amplitude spectrum

Figure 2b shows the amplitude spectrum of a linear chirp signal which has a continuous flat frequency spectrum from DC to 1MHz. However, there are some unwanted ripples in its spectrum. The energy of the sweep in a particular frequency region is not a constant.

Frequency Swept Signal

Constructing the sweep in the frequency domain avoids this problem. The synthesis can be implemented by defining the magnitude and group delay^{[13][14]}:

$$v(t_i) = \sum_{k=f_{start}}^{f_{end}} \cos(2\pi k t_i + \theta_k) \quad (4)$$

where,

$$\theta_k = \theta_{k-1} + (k - f_{start})\Delta\theta \quad (5)$$

$$\Delta\theta = -2\pi / (f_{end} - f_{start}) \quad (6)$$

$$\theta_{f_{start}-1} = 0 \quad (7)$$

Figure 3a shows a synthesized frequency swept signal defined by Equation (4) ~ (7). The synthesized signal has a very flat amplitude spectrum from DC to 1MHz (Figure 3b).

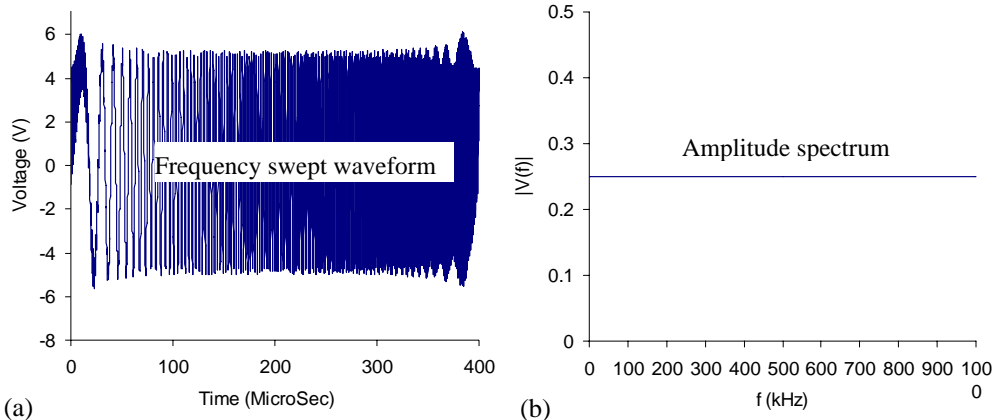


Figure 3 Frequency swept signal: (a) waveform; (b) amplitude spectrums

SIMULATION COMPARISON

To compare these two signal sources for impedance measurement, a simulation for measuring the impedance spectrum of a free PWAS was conducted using the circuit in Figure 4. A low value resistor R_c in series with the PWAS was employed for current measurement. Therefore, the voltage across the PWAS, V_{PWAS} and the current flow through the PWAS, I_{PWAS} in frequency domain are determined by Equation (8) and (9) respectively.

$$V_{PWAS}(f) = \frac{Z_{PWAS}(f)}{Z_{PWAS}(f) + R_c} V_{In}(f) \quad (8)$$

$$I_{PWAS}(f) = \frac{V_{In}(f)}{Z_{PWAS}(f) + R_c} \quad (9)$$

where, Z_{PWAS} designates PWAS impedance. For simplicity, 1-D PWAS model was selected in simulation^[15]:

$$Z_{PWAS}(\omega) = \frac{1}{i\omega \cdot \bar{C}} \left[1 - \bar{k}_{31}^2 \left(1 - \frac{1}{\bar{\varphi} \cot \bar{\varphi}} \right) \right]^{-1} \quad (10)$$

where, ω is the angular frequency, \bar{k}_{31}^2 is the complex coupling factor; \bar{C} is the capacitance of PWAS; $\bar{\varphi}$ is a notation equal $\frac{1}{2}\gamma l$, γ is the wavenumber and l is the PWAS length.

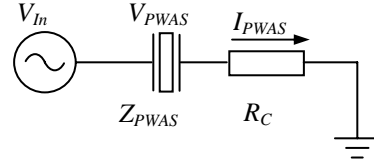


Figure 4 Impedance measurement circuit

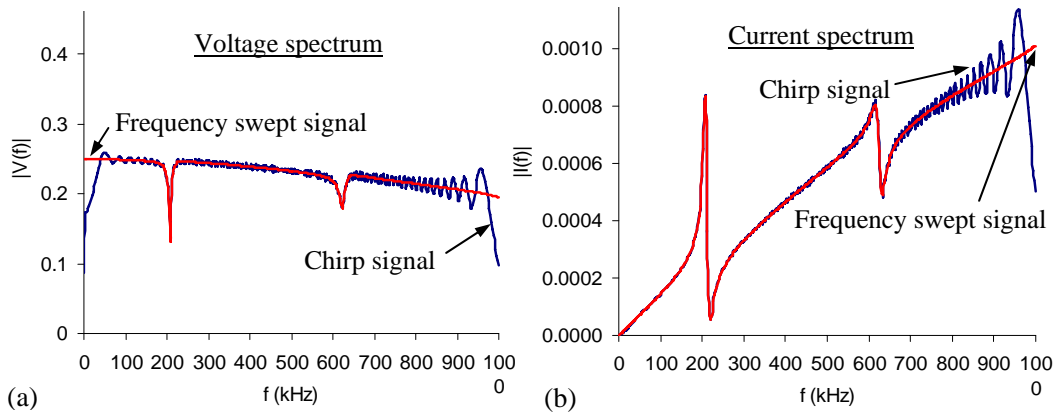


Figure 5 Amplitude spectrum of chirp signal source and frequency swept signal source for free PWAS impedance measurement ($f_s=10\text{MHz}$, $N_{buffer}=4000$, 5Vpp signal source amplitude, $R_c=100\Omega$): (a) voltage spectrum; (b) current spectrum

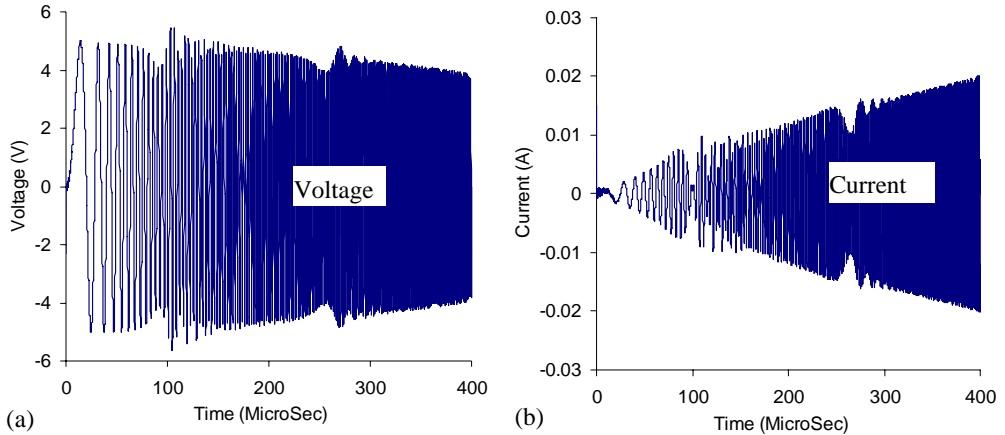


Figure 6 Voltage and current of PWAS using chirp signal source: (a) $V_{PWAS}(t)$; (b) $I_{PWAS}(t)$

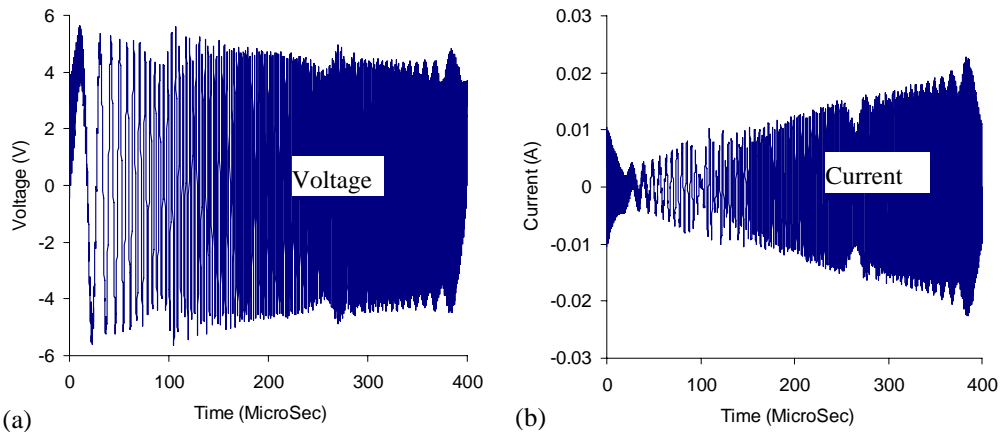


Figure 7 Voltage and current of PWAS using frequency swept signal source: (a) $V_{PWAS}(t)$; (b) $I_{PWAS}(t)$

Equation (8) and (9) permit the calculation of amplitude spectrums of voltage, V_{PWAS} and current, I_{PWAS} (Figure 5). As we can see in Figure 5, there are some ripples in the voltage and current spectrums for chirp signal source, while spectrums for frequency swept signal source are smoother. Due to the change of PWAS impedance at anti-resonance frequency points and also the change of PWAS admittance at resonance frequency points, the first valley in voltage spectrum was observed at the first resonance frequency point, while the first valley in current spectrum was observed at the first anti-resonance frequency point.

Inverse Fourier transforms of Equation (8) and (9) give the voltage $V_{PWAS}(t)$ and current, $I_{PWAS}(t)$ in time domain respectively. Figure 6 and Figure 7 show the waveforms of $V_{PWAS}(t)$ and $I_{PWAS}(t)$ when using chirp signal source and frequency swept signal source as excitations for free PWAS impedance measurement. A comparison of Figure 6b and Figure 7b indicates that frequency swept signal source possesses larger current response than chirp signal source in low frequency range for impedance measurement. Therefore, frequency swept signal source may have higher SNR in low frequency range for impedance measurement.

IMPLEMENTATION AND EXPERIMENTAL RESULTS

Implementation of Novel Impedance Analyzer

The practical implementation of novel impedance measurement system uses the hardware configuration in Figure 8. Digitally synthesized signal sources were first uploaded to non-volatile memory slots of function generator (HP33120A, 12-bit 80MHz internal D/A converter) by using LabVIEW program. The function generator, which was controlled by a PC LabVIEW program via GPIB card, outputs the uploaded excitation with its frequency equal to the frequency resolution (sample rate/buffer size) of the synthesized signal source and its amplitude at 10V peak to peak. The actual excitation and the response of the PWAS were recorded synchronously by a two-channel DAQ card (8-bit, 10MHz sample rate, 4000 points of buffer size). The DAQ card was activated after running of the function generator with a certain amount of delay to ensure the response to stabilize.

The impedance spectrum of the PWAS equals Fast Fourier Transform (FFT) of the excitation over the FFT of the response signal. To improve accuracy and repeatability of measurement, averaging was performed on measurement spectrums instead on time records.

Free PWAS Impedance Spectrum Measurement

Figure 9 and Figure 10 show the superposed results obtained by synthesized sources (chirp signal source and frequency swept signal source) after 256 times of averaging and by using HP4194A laboratory impedance analyzer for measuring the impedance spectrum of a free PWAS (7mm diameter, 0.2mm thickness, APC Inc).

Both of the synthesized signal sources can capture the free PWAS impedance spectrums precisely including the small peaks in the impedance spectrums (Figure 9c&d and Figure 10c&d). For the chirp signal source, small ripples were observed in the voltage and current spectrums in high frequency range (Figure 9a &b). Comparison of the circled parts of impedance spectrums in Figure 9c and Figure 10c showed that frequency swept signal source gave smoother impedance spectrum (Figure 9c) than the one measured by chirp signal source (Figure 10c). This indicates that the frequency swept signal may be the better signal source for impedance spectrum measurement than the chirp signal.

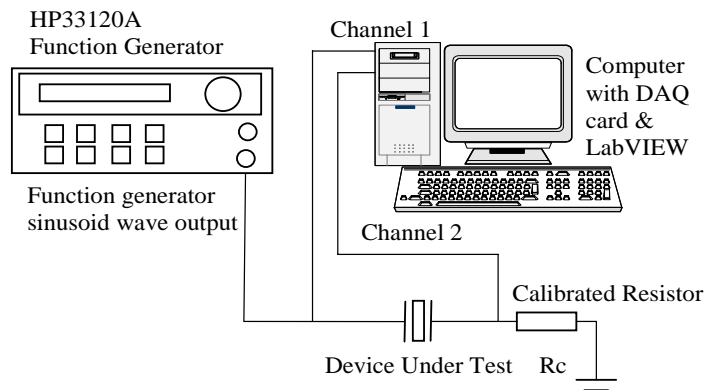


Figure 8 Proof-of-concept demonstration of impedance measurement system

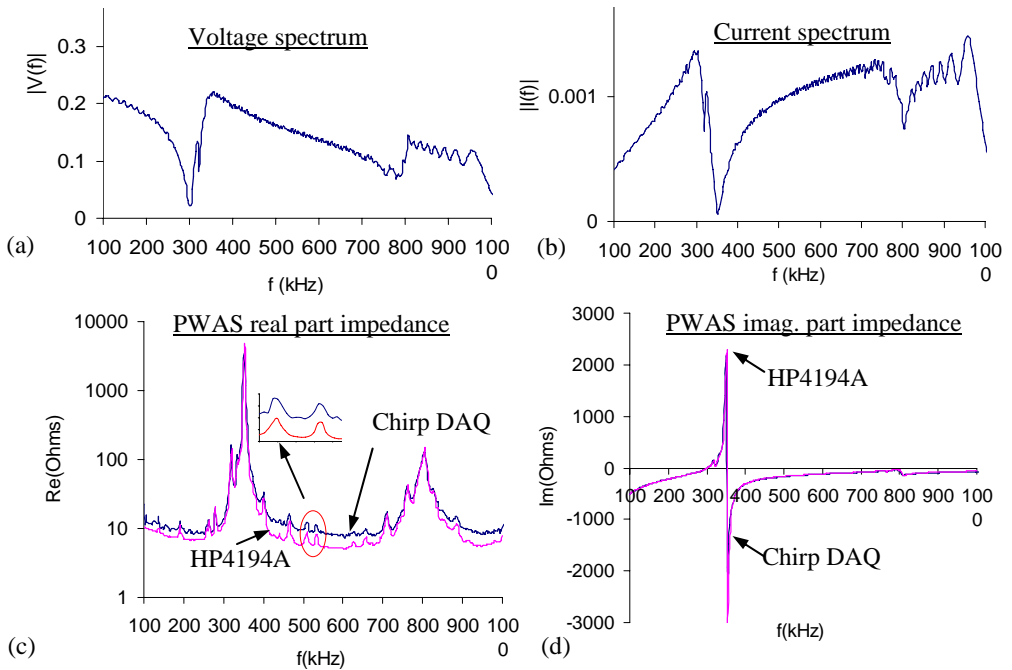


Figure 9 Comparison of PWAS impedance measurement by HP4194A impedance analyzer and using chirp signal source: (a) Amplitude spectrum of voltage across the PWAS; (b) Amplitude spectrum of current; (c) superposed real part impedance spectrum; (d) superposed imaginary part impedance spectrum

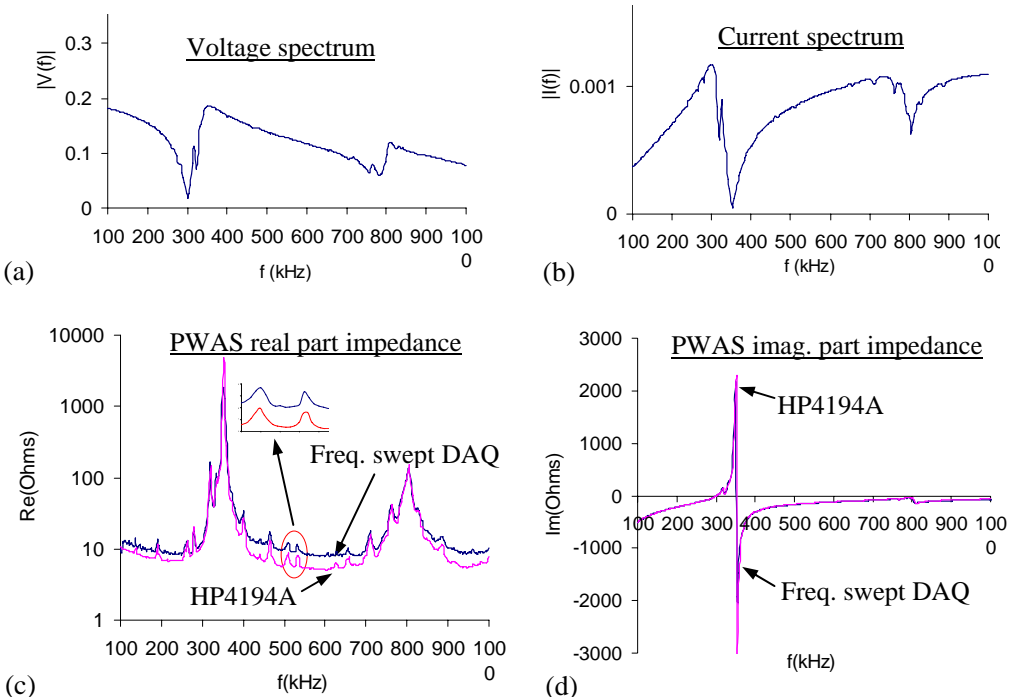


Figure 10 Comparison of PWAS impedance measurement by HP4194A impedance analyzer and using frequency swept signal source: (a) Amplitude spectrum of voltage across the PWAS; (b) Amplitude spectrum of current; (c) superposed real part impedance spectrum; (d) superposed imaginary part impedance spectrum

Spacecraft Panel Disbond Detection By Using E/M Impedance Method

An aluminum test panel was fabricated by NextGen Aeronautics, Inc. The panels consist of the skin (Al 7075, 24x23.5x0.125 in) with a 3 in diameter hole in the center, two spars (Al 6061 I-beams, 3x2.5x0.250 in and 24 in length), four stiffeners (Al 6063, 1x1x0.125 in and 18.5 in length) and fasteners installed from the skin side. The stiffeners were bonded to the aluminum skin using a structural adhesive, Hysol EA 9394. Damages were artificially introduced in the specimen including cracks (CK), corrosions (CR), disbonds (DB), and cracks under bolts (CB). In this experiment, we showed the detection of DB1 (disbond #1, size: 2x0.5 in) by using the novel E/M impedance analyzer and traditional HP4194A impedance analyzer with PWAS a1, PWAS a2, and PWAS a3 (Figure 11).

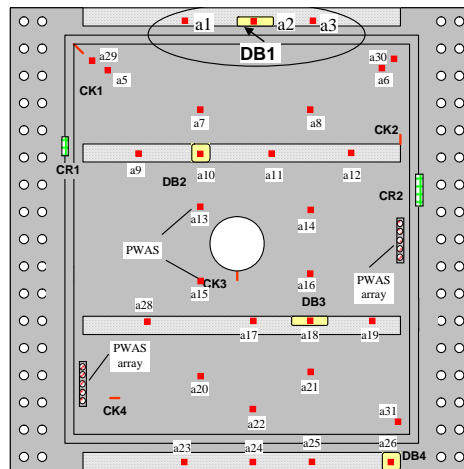


Figure 11 Schematic of the location and the type of the damage on the Panel 1 specimen

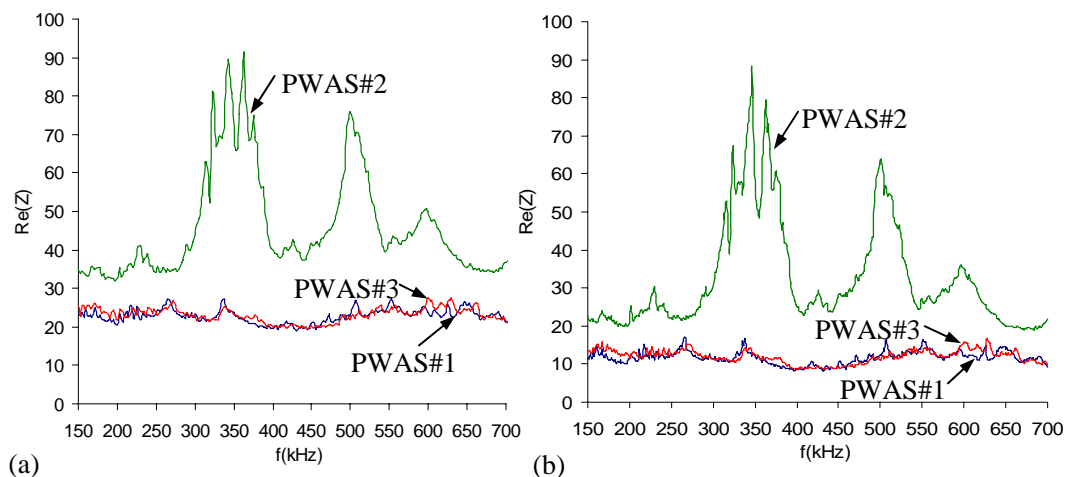


Figure 12 Real part impedance spectrums of PWAS a1, PWAS a2, a3: (a) measured by novel E/M impedance analyzer using frequency swept signal source; (b) measured by HP4194A impedance analyzer

The real part impedance spectrums from PWAS a1, PWAS a2, and PWAS a3 are presented in Figure 12. It can be seen that the impedance spectrums from PWAS a1 and PWAS a3 located on the area with good bond are almost identical. The spectrum from PWAS a2 located on the disbond DB1 is very different showing new strong resonant peaks associated with the presence of the disbond. Both the novel impedance analyzer and HP4194 impedance analyzer can detect the presence of DB1 disbond on the test panel. The peaks in impedance spectrums from novel impedance analyzer match the impedance spectrums from HP4194A impedance analyzer very well.

Even when all precautions have been taken to guarantee a high-precision measurement, it cannot be denied that, unexplainable small differences between the impedance spectrums measured by HP4194A impedance analyzer and the new impedance measurement method. The reasons for these differences are not obvious, although perhaps accuracy of calibrated resistor or terminal configuration may have some effects. For HP4194A impedance analyzer, it is generally equipped with four-terminal configuration (H_c , H_p , L_p and L_c) to interconnect with DUT^[8]. This reduces the effects of lead inductance, lead resistance, and stray capacitance between leads. While the novel impedance analyzer only employs the simple two-terminal configuration.

Also worth noting is that the precision of the new impedance measurement system can be further improved by increasing the buffer size of the system (increasing spectral resolution) or by decreasing the frequency sweeping range in the synthesized signal source (span less while sweeping longer in certain frequency range).

CONCLUSIONS

FFT techniques using sweeps as excitation signals are the most advantageous choice for efficient impedance measurement. The FFT measures the response at all frequencies within the span simultaneously, thus the source must contain energy at all of the measured frequencies. As can be seen in simulation, in the time record, the frequency components in the source add up and the peak source amplitude within the time record exceeds the amplitude of each frequency component by about 26dB (Figure 3, peak source amplitude 5V, amplitude of each frequency component is 0.25V). Since the input range must be set to accommodate the amplitude peak, each frequency component is measured at -26dB relative to full scale. This is why the spectrums of sweep excitation tend to become rather noisy than the one measured by using pure-tone excitations such as HP4194A impedance analyzer. However, this problem can be alleviated by performing averaging of the acquired spectrums over times, by extending the sweep to even longer length to achieve the desired spectral resolution, and by customizing a synthesized signal source which has a desired amplitude spectrum for certain DUT.

Two types of signal sources (chirp signal and frequency swept signal) were synthesized and studied in this paper for efficient impedance measurement. Frequency swept signal source showed slightly better performance for impedance measurement. This was confirmed both in simulation and free PWAS impedance

spectrum measurement experiments. Also, the novel impedance analyzer was successfully used to detect a disbond on an aluminum spacecraft test panel.

The proof-of-concept impedance analyzer was implemented with several pieces of low-cost multipurpose laboratory equipments. By selecting a multifunction DAQ card which has high speed A/D converters and D/A converter integrated, a more compact, field portable, and low-cost computer controlled impedance analyzer can be implemented for structural health monitoring.

ACKNOWLEDGMENTS

Financial supports from NASA South Carolina Space Grant Consortium #520377-3099 and the Air Force Research Lab through UTC Contract #03-S470-033-C1 of F33615-01-D-5801 are thankfully acknowledged.

REFERENCE

1. Giurgiutiu, V.; Zagrai, A. N. (2000a) "Characterization of Piezoelectric Wafer Active Sensors", *Journal of Intelligent Material Systems and Structures*, Vol. 11, pp. 959-976, 2000
2. Park, G., Sohn, H., Farrar, C.R., and Inman, D.J. (2003), "Overview of Piezoelectric Impedance-Based Health Monitoring and Path Forward", *The Shock and Vibration Digest*, Vol. 35, Issue 6, pp. 451-463, 2003
3. Pardo de Vera, C.; Guemes, J. A. (1997) "Embedded Self-Sensing Piezoelectric for Damage Detection," *Proceedings of the International Workshop on Structural Health Monitoring*, September 18-20, 1997, Stanford, CA 445-455
4. Peairs, D.M.; Park, G; Inman, D.J. (2002) "Low Cost Impedance Monitoring Using Smart Materials", *Proceeding of the First European Workshop on Structural Health Monitoring*, Ecole Normale Supérieure, Cachan (Paris), France, July 10-12, 2002
5. Peairs, D.M.; Park, G; Inman, D.J. (2004) "Improving Accessibility of the impedance-Based Structural Health Monitoring Method", *Journal of Intelligent Materials Systems and Structures*, Vol. 15, 129-139, Feb. 2004
6. Giurgiutiu, V.; Xu, B. (2004) "Development of a Field-Portable Small-Size Impedance Analyzer for Structural Health Monitoring using the Electromechanical Impedance Technique", *SPIE's 11th Annual International Symposium on Smart Structures and Materials and 9th Annual International Symposium on NDE for Health Monitoring and Diagnostics*, 14-18 March 2004, San Diego, CA. paper # 5391-923
7. Grisso1, B. L.; Martin, L. A.; Inman1, D. J. (2005), "A Wireless Active Sensing System for Impedance-based Structural Health Monitoring", Proceedings of the IMAC-XXIII:A Conference & Exposition on Structural Dynamics, January 31 – February 3, 2005, Orlando, Florida
8. Agilent Inc., Agilent Technologies Impedance Measurement Handbook, Dec., 2003
9. Macdonald, J. R.(1987), Impedance spectroscopy emphasizing solid materials and systems, John Wiley & Sons, Inc., 1987
10. NI (1993), Application Note 041, "The Fundamentals of FFT-Based Signal Analysis and Measurement in LabVIEW and LabWindows", NI, Nov., 1993
11. Stanford Research Systems (2005), "Model SR780 Network Signal Analyzer-Operating Manual and programming Reference", Revision 2.4, 2005
12. Darowicki, K.; et al (2003), "Continuous-frequency Method of Measurement of Electrode Impedance", *Instrumentation Science & Technology*, Vol 31, No. 1, pp 53-62, 2003
13. Kitayoshi, H.; Sumida, S.; Shirakawa, K.; Takeshita, S. (1985), "DSP Synthesized

Signal Source for Analog Testing Stimulus and New Test Method", 1985 International Test conference, P825-834, 1985

- 14. Muller, S.; Massarani, P., "Transfer-Function Measurement with Sweeps", <http://iem.kug.ac.at/~noisternig/iem/bt2004/ue2/>
- 15. Giurgiutiu, V.; Lyshevski, S. E. (2004a), Micromechatronics Modeling, Analysis, and Design with MATLAB, CRC Press, 2004